Available online at www.sciencedirect.com
ScienceDirect
Polyhedron 26 (2007) 803–810
POLYHEDRON
www.elsevier.com/locate/poly

X-ray structure and multinuclear NMR studies of platinum(II) complexes with 5-methyl-1,2,4-triazolo[1,5-*a*]pyrimidin-7(4*H*)-one

Iwona Łakomska [a,*], Andrzej Wojtczak [a], Jerzy Sitkowski [b,c], Lech Kozerski [b], Edward Szłyk [a]

[a] *Department of Chemistry, Nicholas Copernicus University, Gagarina 7, 87-100 Toruń, Poland*
[b] *National Institute of Public Health, Chełmska 30/34, 00-725 Warsaw, Poland*
[c] *Institute of Organic Chemistry, Polish Academy of Sciences, Kasprzaka 44/52, 01-224 Warsaw, Poland*

Received 25 May 2006; accepted 7 September 2006
Available online 26 September 2006

Abstract

New dichloride platinum(II) complexes with 5-methyl-1,2,4-triazolo[1,5-*a*]pyrimidin-7(4*H*)-one (HmtpO) have been synthesized and characterized by thermal analysis, infrared and ^{1}H, ^{13}C, ^{15}N, ^{195}Pt NMR spectroscopy. X-ray crystal structures of *cis*-$PtCl_2(NH_3)$-(HmtpO) (**1**) and *cis*-$PtCl_2(HmtpO)_2 \cdot 4H_2O$ (**2b**) were determined to $R = 0.0332$ and $R = 0.0802$, respectively. In both complexes the Pt(II) ions have a square-planar geometry with two adjacent corners being occupied by two nitrogens of HmtpO molecules for **2b** or NH_3 and HmtpO molecules for **1**, whereas the remaining adjacent corners are occupied by two chloride anions. Spectroscopic data confirm the square planar geometry with N(3) bonded HmtpO, S-bonded dimethylsulfoxide and two *trans* chloride anions for *trans*-$PtCl_2(dmso) \cdot 4H_2O$ (**3**).
© 2006 Elsevier Ltd. All rights reserved.

Keywords: Platinum complex; 1,2,4-Triazolo[1,5-*a*]pyrimidine derivative; Dimethylsulfoxide; Multinuclear NMR; X-ray structure

1. Introduction

Cisplatin is one of the most commonly used anticancer drugs in the treatment of testicular, ovarian, bladder and head and neck cancer [1,2]. Despite the great success of treating certain kinds of cancer there are several side-effects, and both intrinsic and acquired resistance limit the organotropic profile of the drug [3].

There is a continuing interest in development of new platinum complexes, which are less toxic and have a broader activity spectrum. Variation in the nature of the amine can have a significant effect on the activity and toxicity of these complexes. Several platinum complexes with N-heterocyclic ligands, such as imidazole, thiazole, pyridine and purine derivatives, have been reported [4–7].

Triazolopyrimidine derivatives revealed structures similar to purine, differing from it by the presence of a pyrimidine nitrogen atom in a bridgehead position, and the lack of the acidic H-proton in the five-membered ring [8,9]. Triazolopyrimidine derivatives display a great versatility in their interaction with metal ions, because they can bind metal ions through different sites. Reported studies of triazolopyrimidine complexes display an appreciable variability in their molecular structure. There are examples of mono-, di- and multinuclear structures, which exhibited the central ion and inorganic anions influence on the complex's geometry [10–15]. Nevertheless, when triazolopyrimidines act monodentately to the platinum(II) ion, the preferred binding position appears to be N(3) [12,14]. Mononuclear platinum(II) species such as: *cis*-$PtCl_2$-$(HmtpO)_2 \cdot 2H_2O$ [13], *cis*-$[Pt(HmtpO)_2(NH_3)_2](NO_3)_2 \cdot 2H_2O$ [10] and *trans*-$PtCl_2(dmso)(dmtp)$ [14] revealed N(3) coordinated heterocycles. Polymeric compounds are usually obtained due to N(1) and N(3) coordination [16],

* Corresponding author. Fax: +48 56 654 2477.
E-mail address: dziubek@umk.pl (I. Łakomska).

0277-5387/$ - see front matter © 2006 Elsevier Ltd. All rights reserved.
doi:10.1016/j.poly.2006.09.010

whereas dimers with eight-member rings are formed for the N(3), N(4) bridging mode [10]. The exceptions were complexes with 4,5,6,7-tetrahydro-5,7-dioxo-1,2,4-triazolo[1,5-*a*]pyrimidine (H_2tpO_2), where the bidentate ligands were linked through the exocyclic oxygen O(7) and endocyclic nitrogen N(1) [17].

It was recently demonstrated that the coordination compounds with 1,2,4-triazolo[1,5-*a*]pyrimidine revealed biological activity [13,18–21]. Some transition metal complexes with triazolopyrimidines significantly inhibited in vitro cell growth of the epimastigote [19] and Gram(+) and Gram(−) bacteria. The antitumor activity studies (in vitro) of *cis* platinum(II) compounds with the triazolopyrimidine ligands, 5-methyl-1,2,4-triazolo[1,5-*a*]pyrimidin- 7(4*H*)-one (HmtpO) [13], 5,7-diterbutyl-1,2,4-triazolo[1,5-*a*]pyrimidine (dbtp) [20] and 5,7-diphenyl-1,2,4-triazolo[1,5-*a*]pyrimidine (dptp) [20], indicate a moderate antiproliferative activity against the cells of rectal, breast and bladder cancer.

Following this research line, we have tried to synthesize new platinum(II) compounds, which will reveal activity similar to cisplatin, but have an additional functional group, where they could be linked to carrier substances. Therefore, for our studies we have chosen 5-methyl-1,2,4-triazolo[1,5-*a*]pyrimidin-7(4*H*)-one, with a structure similar to the purine ring existing in DNA, as a ligand for platinum(II). In this paper, we present the results on the synthesis and molecular structure characterization of the novel compounds: *cis*-$PtCl_2$(HmtpO)(NH_3) (**1**), *cis*-$PtCl_2(HmtpO)_2 \cdot H_2O$ (**2a**) and *trans*-$PtCl_2$(HmtpO)(dmso) $\cdot 4H_2O$ (**3**).

2. Experimental

2.1. Materials

Dipotassium tetrachloroplatinum(II), 5-methyl-*s*-triazolo[1,5-*a*]pyrimidine-7-ol (98%), potassium hexafluorophosphate (98%), tetraethylammonium chloride hydrate and tetraphenylphosphonium chloride (98%) were purchased from Aldrich, whereas the inorganic salts and organic solvents of analytical grade were from POCh Gliwice (Poland).

2.2. Instrumentation

The content of C, H, N was determined by elemental semi-microanalysis, Pt spectrophotometrically as H_2PtCl_6 on a Specord M40 Carl Zeiss Jena ($\lambda = 400$ nm). Thermogravimetric analyses were performed with a SDT-2960 TA Instrument (samples – 5 mg, heating range 25–1000 °C, heating rate 3.5 deg/min, N_2 atmosphere). IR spectra were measured with a Perkin–Elmer Spectrum-2000 FT-IR spectrometer, using KBr (400–4000 cm^{-1}) and polyethylene discs (100–400 cm^{-1}). The $^1H\{^{13}C\}$ HSQC, $^1H\{^{13}C\}$ HMBC and $^1H\{^{15}N\}$ HMQC spectra were performed with a Varian INOVA-500 NMR spectrometer equipped with an inverse Nalorac Z-gradient shielded probe. The solvent was dmso-d_6, the concentrations of the saturated solutions were ca. 0.01–0.05 M and the temperature was 298 K. The reference standard was TMS for ^1H and ^{13}C, CH_3NO_2 (external) for ^{15}N and K_2PtCl_6 (external) for ^{195}Pt.

The ^{13}C CPMAS spectra were performed with a Bruker AMX 300 MHz spectrometer using a Bruker MAS-VTN500SB BL4 probe head and 4 mm zirconia rotors, at 296 K.

2.3. Preparation of the platinum(II) complexes

Cis-$PtCl_2(dmso)_2$ [22] and $K[PtCl_3(NH_3)]$ [23] were prepared from K_2PtCl_4 by the known method.

Cis-$PtCl_2(NH_3)$(HmtpO) (**1**): To a solution of $K[PtCl_3(NH_3)]$ (0.050 g, 0.13 mmol) in 10 cm^3 of water, a solution of HmtpO (0.0210 g, 0.13 mmol) in 5 cm^3 of 1 M HCl was added. Reaction mixture was stirred at room temperature for 12 h. The yellow precipitate was filtered, washed with water, acetone, diethyl ether and dried in vacuum. Yield 0.0270 g (48%). *Anal.* Calc. for $C_6H_9Cl_2N_5OPt$: Pt, 45.0; C, 16.6; N, 16.2; H, 2.1. Found: Pt, 44.6; C, 16.7; N, 16.0; H, 1.8%.

Cis-$PtCl_2(HmtpO)_2 \cdot H_2O$ (**2a**): A suspension of K_2PtCl_4 (0.100 g; 0.26 mmol) in 5 cm^3 of water was treated with HmtpO (0.0798 g; 0.53 mmol) in 8 cm^3 of 1 M HCl and the reaction mixture stirred at room temperature for 48 h. The yellow precipitate was filtered, washed with water, acetone, diethyl ether and dried in vacuum. Yield 0.0456 g (30%). *Anal.* Calc. for $C_{12}H_{14}Cl_2N_8O_3Pt$: Pt, 33.4; C, 24.7; N, 19.2; H, 2.4. Found: Pt, 33.0; C, 24.3; N, 19.1; H, 2.6%. The thermal analysis confirmed detachment of water molecule (95–140 °C, weight calc. 3.35%, exp. 3.65%). Further decomposition proceeds in several endothermal stages and leads to metallic platinum above 885 °C. By slow crystallization of **2a** from a mixture of HCl and water (1:3 v/v), single crystals of **2b** suitable for X-ray structure analysis were obtained.

Trans-$PtCl_2(dmso) \cdot 4H_2O$ (**3**): A solution of HmtpO (0.036 g; 0.23 mmol) in 5 cm^3 of 1 M HCl was dropped to a solution of *cis*-$PtCl_2(dmso)_2$ (0.100 g, 0.23 mmol) in 10 cm^3 water–ethanol mixture. The reaction mixture was stirred at room temperature for 24 h. The filtrate was left for crystallization and after 3 days a yellow precipitate was filtered off, washed with ethanol, acetone, diethyl ether and dried in vacuum. Yield 0.0443 g (34%). *Anal.* Calc. for $C_8H_{20}Cl_2N_4O_6SPt$: Pt, 34.4; C, 17.0; N, 9.9; H, 3.6. Found: Pt, 34.1; C, 17.1; N, 9.4; H, 3.9%. The content of solvated water molecules in **3** has been confirmed by thermogravimetric analyses. The first endothermic step in the range 83–272 °C corresponds to the mass loss in the TG curves which can be correlated with detachment of 4 water molecules and dimethylsulfoxide (calc. 26.38%, exp. 26.87%). The next endothermic processes (275–820 °C) can be related to decomposition of **3** leaving platinum as a final product.

2.4. X-ray structure determination

Pale yellow crystals of *cis*-$PtCl_2(NH_3)$(HmtpO) (**1**) and *cis*-$PtCl_2(HmtpO)_2 \cdot 4H_2O$ (**2b**) were obtained by slow evaporation from a mixture of HCl and water. Complex **1** crystallized in monoclinic space group $P2_1/c$, whereas complex **2b** crystallized in the triclinic $P\bar{1}$ space group. The X-ray data for **1** and **2b** were collected at 293(2) K with an Oxford Sapphire CCD diffractometer, using Mo Kα radiation ($\lambda = 0.71073$ Å) and the ω–2θ method. The shape-based numerical absorption correction was applied with minimum and maximum transmissions of 0.04914 and 0.39687 for **1** and 0.17132 and 0.55792 for **2b**. The structure was solved by Patterson methods and refined with the full-matrix least-squares method on F2 with the use of the SHELX-97 program package [24]. The data collection and refinement processes are summarized in Table 1. The residual peaks tabulated for **2b** are positioned 1.16 Å from Cl(1) and 0.86 Å from Pt(1), respectively, therefore not indicating any missing atoms. The fractional coordinates of **1**, **2b** and selected bond lengths and angles are presented in Table 4.

Table 1
Crystal data and structure refinement for **1** and **2b**

Identification code	*cis*-$PtCl_2(NH_3)$-(HmtpO) (**1**)	*cis*-$PtCl_2(HmtpO)_2 \cdot 4H_2O$ (**2b**)
Empirical formula	$C_6H_9Cl_2N_5OPt$	$C_{12}H_{20}Cl_2N_8O_6Pt$
Formula weight	435.15	638.4
Temperature (K)	293(2)	293(2)
Wavelength (Å)	0.71073	0.71073
Crystal system	monoclinic	triclinic
Space group	$P2(1)/c$	$P\bar{1}$
Unit cell dimensions		
a (Å)	9.718(2)	7.121(1)
b (Å)	11.417(2)	10.681(1)
c (Å)	11.138(2)	14.817(2)
α (°)		75.08(1)
β (°)	114.27(3)	76.33(1)
γ (°)		71.64(1)
Volume (Å^3)	1126.5(4)	1018.6(2)
Z	4	2
Calculated density (Mg/m^3)	2.560	2.081
Absorption coefficient (mm^{-1})	12.911	7.198
F(000)	804	616
Crystal size (mm)	$0.40 \times 0.18 \times 0.10$	$0.38 \times 0.28 \times 0.23$
Theta range for data collection (°)	2.68–31.17	2.73–31.18
Index ranges	$-12 \leqslant h \leqslant 13$, $-16 \leqslant k \leqslant 16$, $-15 \leqslant l \leqslant 14$	$-10 \leqslant h \leqslant 9$, $-15 \leqslant k \leqslant 15$, $-21 \leqslant l \leqslant 18$
Reflections collected/ unique [R_{int}]	10821/3403 [0.0524]	10043/5940 [0.1559]
Data/restraints/parameters	3403/0/138	5940/0/264
Goodness-of-fit on F^2	1.095	1.089
Final R indices [$I > 2\sigma(I)$]	$R_1 = 0.0332$, $wR_2 = 0.0796$	$R_1 = 0.0802$, $wR_2 = 0.2228$
R indices (all data)	$R_1 = 0.0388$, $wR_2 = 0.0829$	$R_1 = 0.0863$, $wR_2 = 0.2284$
Largest difference peak and hole (e Å^{-3})	3.299 and −2.074	5.759 and −4.496

2.5. Cytotoxic activity

The antiproliferative activity in vitro against HCV29T (bladder cancer) and T47D (breast cancer) cell lines were performed by using the SRB test as described [20].

3. Results and discussion

3.1. NMR spectroscopy

We have measured ^{1}H, ^{13}C and ^{15}N NMR spectra for **1**, **2a** in solution but not for **3** due to the low solubility of this complex in dmso-d_6 and another solvents. The ^{1}H NMR chemical shifts of the studied complexes are listed in Table 2. The spectra exhibit a singlet at 2.41 (**1**), 2.40 (**2a**) and 2.31 ppm (**3**) for the methyl group and singlets from H(2), H(6) (5.99–8.61 ppm) and H(4) (13.55–13.66 ppm) (Table 2). All signals from H(2), H(6) and H(4) are shifted towards lower fields due to coordination of the triazolopyrimidine ligand. This effect being more expressed for H(2) (0.27–0.44 ppm) and H(4) (0.36–0.44 ppm) than H(6) (0.17–0.26 ppm) (Table 2), suggests slightly stronger deshielding of H(2) and H(4). Therefore the monodentate coordination of HmtpO via N(3) can be proposed, because in the case of the bridging mode (N(3), N(4)), the coordination shifts were bigger (ca. 0.88 ppm) [25]. Additionally, the ^{1}H NMR spectrum of **1** exhibited a broad signal for the NH_3 protons ($\delta =$ 4.06 ppm), which confirms its coordination [26–29].

Coordination sites of the heterocyclic ring were determined by ^{1}H{^{15}N} HMQC spectra of the complexes. In

Table 2
^{1}H and ^{13}C NMR chemical shifts (δ) of the ligand HmtpO and its platinum(II) complexes

Compound	H(6)	H(2)	H(4)	C(2)	C(3a)	C(5)	C(6)	C(7)
HmtpO (in dmso-d_6)	5.82	8.17	13.19	151.7	150.5	151.5	98.0	155.8
(**1**) *cis*-$PtCl_2(NH_3)$(HmtpO)	6.02 (+0.20)	8.44 (+0.27)	13.66 (+0.47)	150.6 (−1.1)	149.8 (−0.7)	153.1 (+1.6)	99.8 (+1.8)	154.5 (−1.3)
(**2a**) *cis*-$PtCl_2(HmtpO)_2 \cdot H_2O$	5.99 (+0.17)	8.61 (+0.44)	13.64 (+0.45)	149.9 (−1.8)	149.5 (−1.0)	152.7 (+1.5)	100.2 (+2.2)	154.4 (−1.4)
(**3**) *trans*-$PtCl_2$(dmso)(HmtpO) $\cdot 4H_2O$	6.08 (+0.26)	8.55 (+0.38)	13.55 (+0.36)	148.3[a] (−1.9)	[b]	153.4[a](+0.7)	101.7[a] (+6.5)	155.9[a] (−1.9)
HmtpO (in the solid state)				150.2	[b]	152.7	95.2	157.8

[a] Data from ^{13}C CPMAS NMR.
[b] The signal was not observed in the spectrum.

the ^{15}N NMR spectra four resonances at: −112.7, −257.3, −251.3, −157.8 for **1** and: −112.1, −257.8, −253.5, −157.9 ppm for **2a** were detected (Fig. 1, Table 3). In comparison to the free ligand spectrum, the shielding effect of N(1), N(3) and N(8) in the complexes is evident, while the biggest coordination shift was observed for N(3) (Δ_{coord} = 91–92 ppm) (Table 3). The strong shielding effect of N(3) is an unambiguous result of N(3) coordination in solution.

^{13}C NMR spectra of **1** and **2a** were recorded, while for **3** no peaks were detectable, due to the low solubility of the latter complex. The signals were assigned by a heterocorrelation ^{1}H–^{13}C technique and data are listed in Table 2. The coordination effect has an impact on C(2) and C(3a) signals which are shielded by 0.7–1.9 ppm in relation to free HmtpO, while C(5) and C(6) resonances are detected 0.7–6.5 ppm towards the low field (Table 2) which can be explained by the deshielding effect of the metal due to coordination via N(3).

A spectrum for complex **3** was measured in the solid phase and data are listed in Table 2. It should be noted that this is the first report of a ^{13}C CPMAS spectrum of HmtpO and one of its platinum(II) complexes. The spectrum presents a similar pattern of coordination shifts as observed in solution (Table 2), which indicates HmptO coordination via N(3). However, the coordination shift of the C(6) signal is larger (maximum 6.5 ppm).

^{195}Pt NMR spectra of **1** and **2a** were measured in dmso-d_6 and data are listed in Table 3. The signals of the *cis*-dichloro complexes were observed at −2089 (**2a**) and −2116 (**1**). These values are at lower field than those

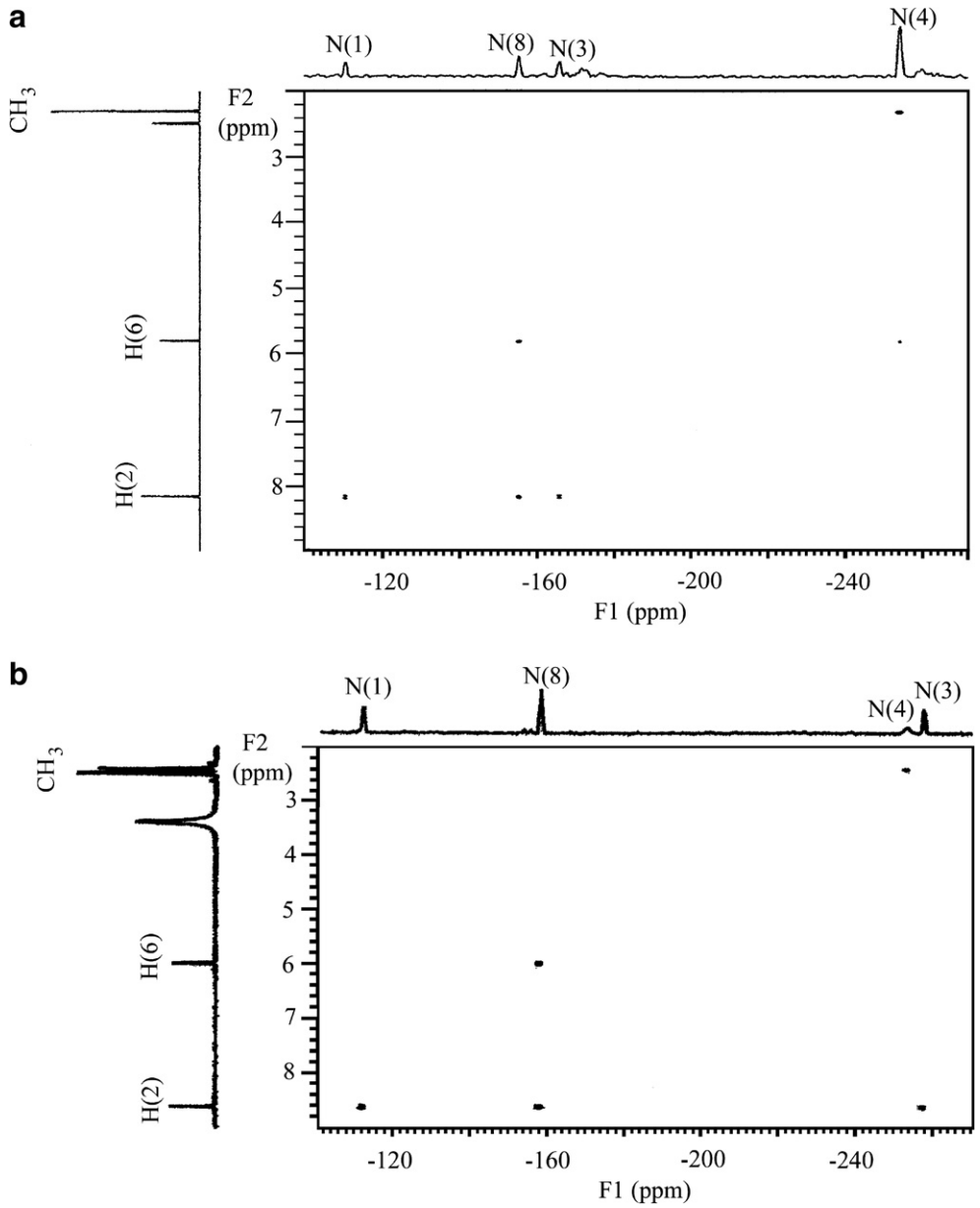

Fig. 1. $^{1}H\{^{15}N\}$ NMR spectra of (a) HmptO; (b) *cis*-$[PtCl_2(HmtpO)_2]\cdot H_2O$ (**1**).

Table 3
^{15}N NMR and ^{195}Pt chemical shifts (δ) of the platinum(II) complexes in dmso-d_6

Compound	N(1)	N(3)	N(4)	N(8)	Pt[a]
HmtpO	−110.8	−165.7	−252.7	−155.3	
(**1**) *cis*-$PtCl_2$(HmtpO)(NH_3)	−112.7 (−1.9)	−257.3 (−91.6)	−251.3 (+1.4)	−157.8 (−2.5)	−2116 (−492)
(**2a**) *cis*-$PtCl_2(HmtpO)_2 \cdot H_2O$	−112.1 (−1.3)	−257.8 (−92.1)	−253.5 (+0.8)	−157.9 (−2.6)	−2089 (−465)

[a] The ^{195}Pt NMR values in parentheses exhibit the chemical shift related to K_2PtCl_4 ($\delta = -1624$ ppm).

reported in the literature for complexes containing amines. This chemical shift range was also observed for other PtN_2Cl_2 chromophore systems [30–32]. In case of Pt(II) complexes containing amines the chemical shifts of ^{195}Pt were noted at: −2188 ppm (Me_2NH), −2224 ppm (*i*-$PrNH_2$), −2104 ppm (NH_3), −2184 ppm (1-adamantanamine), −2235 ppm (cyclobutyloamine) (in dmf-d_7) [33], whereas for *cis*-pyridine derivatives the chemical shifts were between −1998––2021 ppm (in $CDCl_3$) [34]. However, the resonances for the complexes with triazolopyrimidine derivatives are observed at lower field than those reported in the literature for complexes containing aromatic amines. The low field shift of ^{195}Pt signals can be related to a smaller σ electron donation effect in triazolopyrimidine ligands than in aliphatic amines complexes. This phenomenon can cause a reduction of electron density on the Pt(II) nuclei, resulting in its deshielding and larger ^{195}Pt signal coordination shift.

3.2. IR spectra

Absorption bands of ν(C=O) stretching vibrations at 1724 (**1**), 1709 (**2a**), 1714 cm^{-1} (**3**) upon coordination were shifted towards higher frequencies (max. 23 cm^{-1}). In addition, the two most characteristic bands of pyrimidine and imidazole ring skeleton vibrations after coordination appeared at higher frequencies by 18–30 cm^{-1} and 11–19 cm^{-1}, respectively. A similar effect has been already found for other complexes with N(3) coordinated triazolopyrimidine derivatives [13,14,20].

Table 4
Selected bond lengths (Å) and angles (°) for *cis*-$PtCl_2(NH_3)$(HmtpO) (**1**) and *cis*-$PtCl_2(HmtpO)_2 \cdot 4H_2O$ (**2b**)

Bond/angle	**1**	**2b** Ligand I	**2b** Ligand II
Pt(1)–N(3)	2.022(4)	2.059(8)	2.052(9)
Pt(1)–N(21)	2.029(5)		
Pt(1)–Cl(1)	2.2667(15)	2.276(3)	
Pt(1)–Cl(2)	2.2971(16)	2.290(3)	
C(2)–N(3)	1.355(7)	1.355(14)	1.350(13)
N(3)–C(3A)	1.323(6)	1.293(13)	1.286(12)
N(3)–Pt(1)–N(21)	91.7(2)	92.2(3)	
N(3)–Pt(1)–Cl(1)	176.13(13)	178.9(2)	87.6(2)
N(21)–Pt(1)–Cl(1)	87.30(16)		
N(3)–Pt(1)–Cl(2)	89.57(14)	87.8(3)	179.3(2)
N(21)–Pt(1)–Cl(2)	177.49(16)		
Cl(1)–Pt(1)–Cl(2)	91.60(7)	92.30(14)	
C(3A)–N(3)–Pt(1)	129.7(3)	124.3(8)	127.7(7)
C(2)–N(3)–Pt(1)	125.6(3)	126.8(8)	124.9(7)

In the spectrum of **3**, two new intensive absorption bands were detected at 1135 and 1024 cm^{-1}, which can be assigned to ρ_{CH3} rocking vibrations and ν_{SO} stretching vibration, respectively [22,35]. Similar bands were noted in the spectra of *trans*- and *cis*-$PtCl_2$(thiazole)(dmso) where S-bonded dmso was postulated (1150 and 1140 cm^{-1}, respectively) [29,36]. Recently, we have found a ν_{SO} band in the spectra of *trans*-$PtCl_2$(dmso)L complexes (L = 1,2,4-triazolo[1,5-*a*]pyrimidine or its 5,7-disubstituted derivatives), at similar frequencies (1142–1147 cm^{-1}) [14].

From group theory calculations, for a C_{2v} coordination sphere geometry ($PtCl_2N_2$) two of each stretching vibrations of Pt–Cl and Pt–N should of A_1 and B_1 type, all active in IR spectra. Far-IR spectra of complexes **1**–**3** exhibit one broad band of medium intensity, which can be assigned to Pt–Cl vibrations (A_1) (332–342 cm^{-1}). In the spectra of **1** and **2a** the second band appeared as a shoulder, due to coincidence with the ligand normal oscillations. However, the frequencies of the ν(Pt–Cl) bands in the spectra of the studied complexes were in the range characteristic for the *cis* geometry. In the case of platinum(II) complexes with HmtpO one broad band was reported at 330 cm^{-1} [13]. Similar complexes with 1-(2-aminophenyl)isoquinoline derivatives exhibit the band in the range 328–335 cm^{-1} [7], whereas those with substituted benzimidazole derivatives between 337 and 312 cm^{-1}, which is consistent with the values reported in this work [37].

3.3. Crystal structure of *cis*-$PtCl_2(NH_3)$(HmtpO) (**1**)

The crystal structure of **1** is formed by *cis*-$PtCl_2(NH_3)$-(HmtpO) units. The atom numbering scheme of **1** is shown in Fig. 2.

The coordination sphere of **1** is formed by the ammine and HmtpO ligand bonded in *cis* positions and two chloro ligands. The rms deviation of the atoms from the best PtN_2Cl_2 plane is 0.05 Å. The HmtpO ligand is coordinated via the N(3) atom, the Pt–N distance being 2.022(4) Å. The ammonia N(21) atom forms a 2.029(5) Å bond to platinum(II). The chloro ligands form Pt–Cl(1) and Pt–Cl(2) bonds of 2.267(2) and 2.297(2) Å, respectively, as expected for such bonds. The slight elongation of Pt–Cl2 might result from the *trans* influence of the ammine ligand and the steric effect of the HmtpO ligand being stronger than that of the ammine ligand. That conclusion is supported by the observed value of the N(3)–Pt(1)–Cl(2) angle 89.6(1)°, slightly larger than that of 87.3(2)° found for N(21)–Pt(1)–Cl(1).

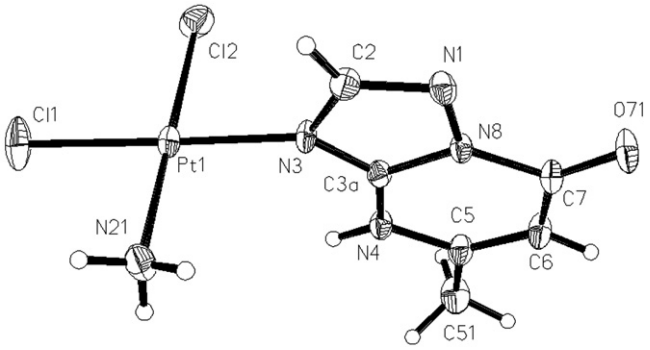

Fig. 2. Molecular structure of compound **1** as determined from X-ray diffraction data.

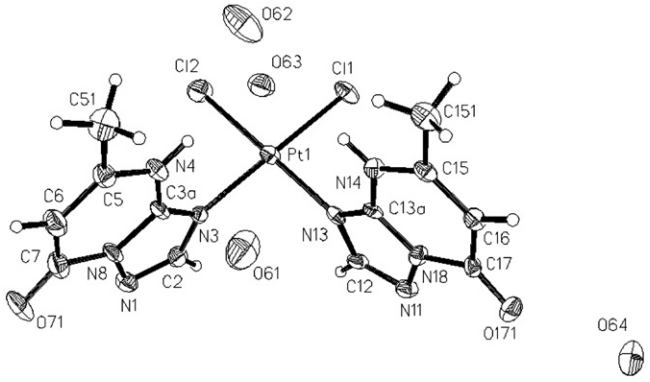

Fig. 3. Molecular structure of compound **2b** as determined from X-ray diffraction data.

The HmtpO ligand is planar, the rms deviation of the atoms from the best plane is 0.0127 Å. However, there is a slight bend of the ring system along the N(8)–C(3a) bond, the angle between the triazole ring and pyrimidine ring planes being 1.1(4)°. The HmtpO ring system is almost perpendicular to the PtN_2Cl_2 plane, the dihedral angle being 88.97°.

The intermolecular interactions in the crystal lattice include a network of hydrogen bonds formed by all donor N–H groups of the ligands. The ammine ligand N(21) forms H-bonds to Cl(2) $[-x+1, y+1/2, -z+3/2]$, O(71) $[x+1, y, z]$ and Cl(1) $[x, -y+1/2, z+1/2]$ atoms (N···Cl/O distances of 3.430, 3.103 and 3.244 Å, respectively). N(1)–H participates in the 2.904 Å contact with N(4) $[x, -y+1/2, z+1/2]$. The C(2)–H and C(6)–H groups form almost linear interactions to chloride ions, C(2)···Cl(2) $[1-x, -y, 2-z]$ and C(6)–H(6A)···Cl(2) $[-x, 0.5+y, 1.5-z]$ being 3.579(6) and 3.551(6) Å, respectively. The corresponding H(2A)···Cl(2) and H(6A)···Cl(2) distances are 2.67 and 2.64 Å, while the C(2)–H(2A)···Cl(2) and C(6)–H(6A)···Cl(2) angles are 165.9° and 167.5°, respectively. Such C–H···Cl interactions have been reported for other complexes of 1,2,4-triazolo-[1,5-*a*]pyrimidines [14] and indicate the significant polarization of these C–H bonds.

3.4. Crystal structure of *cis*-$PtCl_2(HmtpO)_2 \cdot 4H_2O$ (**2b**)

Cis-$PtCl_2(HmtpO)_2 \cdot 4H_2O$ molecules form the crystal structure of **2b**. The atom numbering scheme is shown in Fig. 3.

The structure of the new form of *cis*-$[PtCl_2(HmtpO)_2] \cdot 4H_2O$ (**2b**) was solved in the triclinic $P\bar{1}$ space group. A similar X-ray structure of $[PtCl_2(HmtpO)_2]$ dihydrate was solved in the monoclinic $P2_1/c$ space group with poor diffraction data [13]. However, the authors reported problems with the refinement of the second HmtpO ligand and explained the poor data quality by crystal dehydration during the experiment. Analysis of that paper revealed that one of the HmtpO ligands had a significant disorder, which resulted in its isotropic refinement and large values of the reported atomic displacement parameters, being 5 times the average value for the other HmtpO ligand. Also, authors commented that the poor quality data did not allowed any discussion of the ligand geometry [13]. Therefore, we decided to re-determine the structure of **2b** because of its biological significance and compare it with the structure of **1**. The crystal of **2b** was taken out from the solution and immediately mounted on the diffractometer for a fast experiment with the CCD detector. The reported structure contains four independent water molecules, two of which reveal slightly larger atomic displacement parameters than the other two. That might indicate the ability of the crystal to partially dehydrate and also a possible change of the lattice symmetry. However, the analysis of the experiment does not reveal the possible choice of the monoclinic cell corresponding to the dihydrated complex [13]. Furthermore, the quality of the new triclinic form of the hydrated *cis*-$[PtCl_2(HmtpO)_2] \cdot 4H_2O$ structure (**2b**) reported here is much better than that of the monoclinic form determined by the other authors [13]. Partial dehydration would be consistent with the difficulties of getting high quality diffraction data, we tried several crystals (with relatively high R_{int}), as reported by the other group [13].

Similar to the lower quality complex structure, the coordination sphere is formed by two *cis* chloride ions and two HmtpO ligands bonded to the Pt atom via N(3) atoms [13]. The Pt(1)–Cl(1) and Pt(1)–Cl(2) distances observed in **2b** are 2.276(3) and 2.290(3) Å, respectively and are similar to the analogous distances in complex **1**. The Pt(1)–N(3) and Pt(1)–N(13) distances are 2.059(8) and 2.052(9) Å, respectively and are slightly longer than those found in **1**. The HmtpO ligands are oriented in the same way with respect to the chloride ligands (Fig. 3). Such a position results from the pair of H-bonds formed by the N(4)–H groups to water O(63).

The HmtpO ligands are planar, the rms deviation of the atoms from the best plane is 0.013 and 0.019 Å for the N(1)–N(8) and N(11)–N(18) ligands, respectively. The dihedral angle between the best planes of these two ligands is 70.3(2)°. The corresponding value reported for the

Table 5
Structural differences between mononuclear Pt(II) complexes with triazolopyrimidines

Compounds	Bond distances (Å)		Angles (°)		Ref.
	Pt–N(3)	Pt–Cl	L–Pt–N(3)	Pt–N(3)–C(3A)	
cis-$PtCl_2(HmtpO)_2 \cdot 2H_2O$	2.00(2) 1.98(2)	2.278 (6) 2.274(8)	91.7(4) 89.7(7) 178.5(6) 177.3(4)	129(1) 130(2)	[13]
cis-$[Pt(NH_3)_2(HmtpO)_2](NO_3)_2 \cdot 2H_2O$	2.018(8) 2.012(8)		88.0(3) 90.9(3) 90.6(3) 90.7(3) 176.6(3) 176.3(3)	127.0(6) 129.5(7)	[25]
trans-$PtCl_2$(dmtp)(dmso)	2.048(5)	2.295(2) 2.303(2)	87.63(15) 89.2(2) 176.9(2)	[a]	[14]

[a] Data unavailable.

monoclinic form [13] was 79.8°, and has been strongly affected by the reported HmtpO ring disorder. The dihedral angles formed between the coordination PtN_2Cl_2 plane and HmtpO ring systems are 82.0(2) and 73.4(2)° for N(1)–N(8) and N(11)–N(18) ligands, respectively. The bend of the HmtpO ring system along the N(8)–C(3a) bond is similar to that detected in **1**. The dihedral angle between the triazole ring and pyrimidine ring planes are 1.2(8) and 2.2(6)° for N(1)–N(8) and N(11)–N(18) ring systems.

The intermolecular interactions include the network of H-bonds formed by N(1)–H(1A)···O(64) $[-x-1,-y,-z+1]$, N(4)–H(4A)···O(63) and N(14)–H(14A)···O(63), the corresponding N···O distances being 3.025(2), 2.788(2) and 2.854(2) Å. The water molecules also interact with other waters and chloride ions, although lack of hydrogen atoms in the model does not allow a discussion of the details of those interactions. One C–H···Cl interaction was found, that is analogous to those described for **1**. That is C(12)–H(12A)···Cl(1) $[-x,-y,1-z]$ with a C···Cl distance of 3.693(11) Å and C–H···Cl angle of 173.2°. The series of stacking interactions between the ring systems of the neighboring molecules complete the packing interactions.

Table 5 presents the main structural differences between known mononuclear Pt(II) complexes with triazolopyrimidines. Careful interpretation has shown that the Pt–N and Pt–Cl distances are not significantly different, but the Pt–N bond seems slightly longer when it is in a *trans* position to the chloro ligands. These results indicate that the *trans* influence of the chloro and triazolopyrimidine ligands is very similar and it might be greater for chloro ligands. However, more X-ray data are needed to determine with a bigger probability that the *trans* impact of the chloro ligands is larger than the influence of the heterocyclic ligands.

3.5. Cytotoxic activity

Many transition metals complexes with triazolopyrimidines show significant antitumor activity [13,20]. We have observed high activity of similar platinum(II) complexes with analogs of HmtpO (e.g 5,7-diphenyl-1,2,4-triazolo[1,5-*a*]pyrimidine (dptp) and 5,7-diterbutyl-1,2,4-triazolo[1,5-*a*]pyrimidine (dbtp) [20]). The in vitro antiproliferative activity of the studied platinum compounds **1**, **2a** was determined against two human cell lines: T47D (breast cancer) and HCV29T (bladder cancer). However, the obtained results indicate that studied platinum complexes are not cytotoxic in the concentration range 0.1–100 μg/ml.

4. Conclusion

The molecular structure and antiproliferative activity in vitro of mononuclear platinum(II) complexes with HmtpO were studied. The observed coordination mode via N(3) may be regarded as representative for triazolopyrimidines and analogous to N(9) complexation in purine. The crystal structures of **1**, **2b** indicate that the Pt(II) ion has a square planar geometry with N(3) bonded HmtpO, N-bonded second ligand (NH_3 (**1**) and HmtpO (**2b**)) and two *cis* chloride anions.

The results of the human cancer cell lines treatment with the new platinum(II) complexes confirm lower cytotoxicity of these compounds than cisplatinum in the concentration range 0.1–100 μg/ml.

5. Supplementary material

CCDC 276404 and 276405 contain the supplementary crystallographic data for **1** and **2b**. These data can be obtained free of charge via http://www.ccdc.cam.ac.uk/conts/retrieving.html, or from the Cambridge Crystallographic Data Centre, 12 Union Road, Cambridge CB2 1EZ, UK; fax: (+44) 1223-336-033; or e-mail: deposit@ccdc.cam.ac.uk.

Acknowledgment

Financial support from Polish Committee for Scientific Research (KBN) Grant No 4 T09A 11623 is gratefully acknowledged.

References

[1] P.J. O'Dwyer, J.P. Stevenson, S.W. Johnson, in: B. Lippert (Ed.), Cisplatin in Chemistry and Biochemistry of a Leading Anticancer Drug, Wiley-VCH, Weinheim, 1999, p. 31.
[2] J. Reedijk, Chem. Rev. 99 (1999) 2499.
[3] E.R. Jamiesion, S.J. Lippard, Chem. Rev. 99 (1999) 2467.
[4] L.R. Kelland, in: B. Lippert (Ed.), Cisplatin in Chemistry and Biochemistry of a Leading Anticancer Drug, Wiley-VCH, Weinheim, 1999, p. 498.
[5] K.A. Skov, H. Adomat, M. Doedee, M. Farrell, Anti-Cancer Drug Des. 9 (1994) 103.

[6] N. Farrell, T.B.T. Ha, J.P. Souchard, F.L. Wimmer, S. Cros, N.P. Johnson, J. Med. Chem. 32 (1989) 2240.
[7] F. von Nussbaum, B. Miller, S. Wild, Ch.S. Hilger, S. Schumann, H. Zorbas, W. Beck, W. Steglich, J. Med. Chem. 42 (1999) 3478.
[8] G. Fischer, Z. Chem. 30 (1990) 305.
[9] G. Fischer, Adv. Het. Chem. 57 (1993) 81.
[10] J.A.R. Navarro, M.A. Romero, J.M. Salas, M. Quirós, E.R.T. Tiekink, Inorg. Chem. 36 (1997) 4988.
[11] M.A. Haj, M. Quiros, J.M. Salas, R. Fure, Inorg. Chem. Commun. 4 (2001) 254.
[12] A.H. Velders, F. Ugozzoli, M. Biagini-Cingi, A.M. Montti-Lanfredi, J.G. Haasnoot, J. Reedijk, Eur. J. Inorg. Chem. 2 (1999) 213.
[13] J.A.R. Navarro, J.M. Salas, M.A. Romero, R. Vilaplana, F. Gonzáles-Vilchez, R. Faure, J. Med. Chem. 41 (1998) 332.
[14] E. Szłyk, I. Łakomska, A. Surdykowski, T. Głowiak, L. Pazderski, J. Sitkowski, L. Kozerski, Inorg. Chim. Acta 333 (2002) 93.
[15] K. Akdi, R.A. Vilaplana, S. Kamah, J.A.R. Navarro, J.M. Salas, F. Gonzalez-Vilchez, J. Inorg. Biochem. 90 (2002) 51.
[16] J.A.R. Navarro, M.A. Romero, J.M. Salas, R. Faure, X. Solans, J. Chem. Soc., Dalton Trans. 6 (1997) 1001.
[17] S. Orihuela, M.P. Sanchez, M. Quiros, D. Martin, R. Faure, Polyhedron 17 (1998) 2477.
[18] F. Luque, C. Fernández-Ramos, E. Entrala, M.J. Rosales, M.C. Salas, J. Navarro, M. Sánchez-Moreno, Toxicol. in Vitro 14 (2000) 487.
[19] F. Luque, C. Fernández-Ramos, E. Entrala, M.J. Rosales, J.A. Navarro, M.A. Romero, J.M. Salas, M. Sánchez-Moreno, Comp. Biochem. Physiol. C 126 (2000) 39.
[20] I. Łakomska, E. Szłyk, J. Sitkowski, L. Kozerski, J. Wietrzyk, M. Pełczyńska, A. Nasulewicz, A. Opolski, J. Inorg. Biochem. 98 (2004) 167.
[21] M.A. Romero, J.M. Salas, M. Quiros, D.J. Williams, J. Molina, Transition Met. Chem. 18 (1993) 595.
[22] J.H. Price, A.S. Williamson, R.S. Schramm, B.B. Wayland, Inorg. Chem. 11 (1972) 1280.
[23] E.G. Tolman, W. Brüning, J. Reedijk, A.S. Spek, N. Veldman, Inorg. Chem. 36 (1997) 854.
[24] G.M. Sheldrick, T.M. Schneider, Methods Enzymol. B 277 (1997) 319.
[25] J.A.R. Navarro, M.A. Romero, J.M. Salas, M. Quiros, Inorg. Chem. 36 (1997) 3277.
[26] M. van Beusichem, N. Farrell, Inorg. Chem. 31 (1992) 634.
[27] G. Annibale, M. Bonivento, L. Cattalini, M.L. Tobe, J. Chem. Soc., Dalton Trans. 24 (1992) 3433.
[28] C. Sacht, M.S. Datt, S. Otto, A. Roodt, J. Chem. Soc., Dalton Trans. 5 (2000) 727.
[29] O. Clement, A.W. Roszak, E. Buncel, Inorg. Chim. Acta 253 (1996) 53.
[30] P.S. Pregosin, Coord. Chem. Rev. 44 (1982) 247.
[31] P.S. Pregosin, Transitions Metal Nuclear Magnetic Resonance, Elsevier, Amsterdam, 1991, p. 217.
[32] F.D. Rochon, A. Morneau, Magn. Res. Chem. 29 (1991) 120.
[33] F.D. Rochon, M. Doyon, I.S. Butler, Inorg. Chem. 32 (1993) 2717.
[34] Ch. Tessier, F.D. Rochon, Inorg. Chim. Acta 295 (1999) 25.
[35] F.A. Cotton, R. Francis, W.D. Horrocks, J. Chem. Soc. 64 (1960) 1534.
[36] A. Corina, A.C. Fabretti, M. Bonivent, L. Cattalini, Inorg. Chim. Acta 255 (1997) 405.
[37] F. Gümüş, I. Pamuk, T. Özden, S. Yildiz, N. Diril, E. Öksüzoğlu, S. Gür, A. Özkul, J. Inorg. Biochem. 94 (2003) 255.